BANDPASS SIGNAL PROCESSING

J. HALÁMEK, M. KASAL
Institute of Scientific Instruments, AV ČR
Královopolská 147, 612 64 Brno
M. VILLA, P. COFRANCESCO
Dipartimento di Fisica "A. Volta", Universitá di Pavia
Via Bassi 6, I-27100 Pavia, Italy

Abstract

We present the bandpass signal analysis based on digital receiver and call attention to the aliasing of the complex signal, the digital quadrature detector when sampling is equal to quadruple of the carrier frequency, and frequency response of narrow lowpass filters. The design of the digital receiver is described and some results of measurements are presented.

1. Introduction

An analysis of the bandpass signal is a common requirement in many areas (communication, radar, spectroscopy, control ...). The analysis is based on frequency conversion (mostly quadrature detection) and low pass filtering. An analog or digital solution may be used. A pioneering and beautiful application of the digital solution, the digital quadrature detection (**DQD**) and digital filtering (**DF**) in real time, was the analyzer HP3582, described by Hewlett-Packard in 1978 [1]. Its design was based on custom VLSI IC, and the input frequency was limited to the audio band. This processing was named **ZOOM FFT**. Since then, many design have been described with the aim to increase the frequency band or to simplify the hardware. The analog quadrature detection or frequency conversion based on undersampling or time shifted sampling was used. The disadvantages of such a design were that the analog processing of dc signals had to be made and that the output real and imaginary parts of the signal were mostly not quite symmetric. As a result, ghost signals and a worse signal to noise ratio (SNR) take place. Only recently digital designs were presented that can be used for a high sampling frequency [2-7].

At present, the semiconductor technology involves the levels of the integration and processing speed required for the implementation of a digital receiver in a single IC [3,4]. The leading firm in this area is HARRIS Semiconductor. Its special Digital Signal Processor (**DSP**) for communication can be used in many areas. This DSP are an ideal solution of the narrow low pass filtering, and DQD and the basic applications are nearly without problems. But in the areas where a large dynamic range of signals (> 80 dB) or an analysis of transient response is needed some problems may occur - the baseline distortion or ghost signals [8-10]. Only if we understand well all problems, we can make full use of all the advantages of the digital signal processing that include the resulting signal without ghost signals and distortions and with a nearly ideal SNR.

2. Bandpass Signal

A continuous-time signal $x(t)$ with the frequency content concentrated in a narrow band of frequencies around some centre frequency F_c *(carrier frequency)* is called the *bandpass signal* and can be given by

$$x(t) = A(t)\cos(2\pi F_c t + \Phi(t)) \qquad (1)$$

where $A(t)$ is the amplitude or envelope and $\Phi(t)$ is the phase. By defining the *complex envelope* $u(t)$

$$u(t) = u_c(t) + j\,u_s(t) = A(t)\,[\cos(\Phi(t)) + j\sin\Phi(t))] \qquad (2)$$

we receive:

$$x(t) = RE[\,u(t)\exp(j\,2\pi F_c t)\,] \qquad (3)$$

So any bandpass signal $x(t)$ can be represented by an equivalent lowpass signal $u(t)$. The aim of the processing of the bandpass signal is to receive the complex envelope $u(t)$. The first step, the quadrature detection (**QD**), is the multiplication by the harmonic complex signal with the frequency $-F_c$. The second step is the lowpass filtering which cuts off the signals round the frequency $-2F_c$, and the result is the complex envelope $u(t)$. The representation in the frequency domain of this processing is shown in Fig. 1. The input signal is sampled using the frequency F_s, and we must count with the periodicity of the spectrum. The corresponding block diagram is shown in Fig. 2. The basic blocks are the DQD and narrow lowpass filters. The input analog bandpass filter warrants that $x(t)$ has no frequency components near $f=0$ and above $F_s/2$.

3. Digital Quadrature Detection

The DQD is the multiplication of the input real samples $x(t)$ by sin and cos signals. The output is the real Rn and the imaginary In set of samples. The frequency band of the output signal is $(-F_s/2, F_s/2)$ and there is no symmetry between positive and negative frequencies any longer.

For the generation of the needed multiplicands the quadrature output of a direct digital synthesizer (**DDS**) can be used. This approach requires an analysis of the rounded off errors from DDS and multipliers and may be a source of spurious signals.

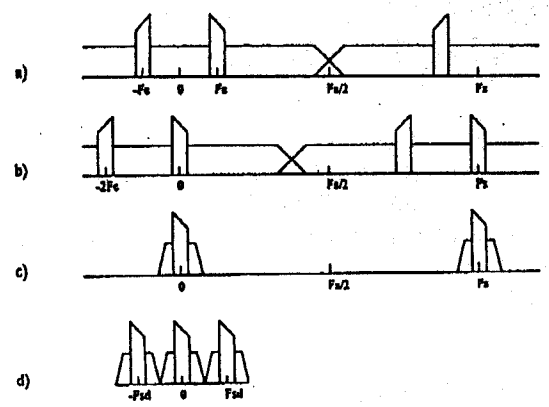

Fig. 1. Digital bandpass signal processing. a) Spectrum of the input signal b) Spectrum after DQD c) Spectrum after lowpass digital filtering d) Spectrum of the output signal, after sample decimation

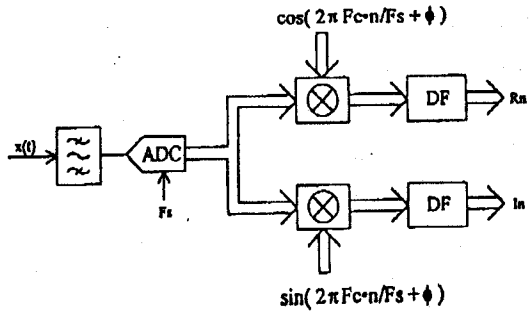

Fig. 2. Basic block diagram.

In some application, a fixed relation between the sampling and carrier frequency can be supposed. The solution when the sampling is equal to the quadruple of the carrier frequency, $Fs = 4Fc$, simplifies the hardware, and also rounding errors disappear and so DQD does not limit the dynamic range of the analyzed signal. In this way, the argument of sin and cos increases in steps of $\pi/2$; with $\Phi=0$, the sequence of the coefficients is *{1, 0, -1, 0,...}* in the real channel, and *{0, 1, 0, -1,...}* in the imaginary channel (case A). With $\Phi = \pi/4$ and normalization, the coefficients *are {1, -1, -1, 1,...}* and *{1, 1, -1, -1,...}* (case B). Some other data, the so called *Redfield data* (or *Redfield-Kunz data*) [11,12], are the data with $\Phi=0$ where the samples with zero multiplicands are omitted. In this case we have a decimated set of output samples, and the samples in the real and the imaginary channel are mutually shifted by time $T/2$, where $T=1/Fs$. This data was first used by Redfield [12] in the design of the NMR receiver with an analog quadrature detector and one ADC.

From this it is obvious that in the simplest example of DQD there can be three different output data sets. The cases A and B do not differ too much, there is no time shift between the real and the imaginary channel. The difference is only the phase shift of the output signal. This can have a influence only in the case of the special data processing or marked ADC jitter. The time shift between the real and the imaginary channel in the case of Redfield data is more serious. In NMR spectroscopy, there are many articles that discuss which type of data is better from the point of view of the resulting spectral distortion. But no proper analysis has been made as to where the origin of the difference is. When simplifying the hardware of the real time digital filters and making frequency conversion using undersampling or time shifted sampling, also a general time shift dT between the real and the imaginary set of the output samples can occur [2,6]. This data can be called *complex-dT data*.

The theoretical analysis of the influence of the time shift has not been made. It was only assumed, that the aliasing does not occur during the sampling and data processing. This means also during the sample decimation used with the digital filtering. So $F_{max}<F_s/2$ must be valid. It is very difficult to fulfil this condition in case of the real measurement. This can be fulfilled in measurements with a low dynamic range and where it does not depend on the data block size only. So at most measurements we must count with the aliasing and in this case also with the influence of the used time shift. The influence of dT on aliasing signals is the explanation of different ghost signals and baseline distortions that occur for different data types [9].

4. Sampling and aliasing of complex data

The complex signal, sampled using the frequency F_s, has the frequency band $(-fs/2, fs/2)$. It does not depend on the time shift between the real and the imaginary part, as long as the proper processing is used. An example of the proper FFT algorithm is given in the appendix. The situation is different when the signals are outside the Nyquist band. The position and phase of the aliasing signals are functions of the time shift.

To analyze the effect of aliasing signals, we assume that the sampled harmonic signal has the frequency F_a in the band $(F_s/2, F_s)$. So owing to the sampling this signal will be aliased in the base band $(-F_s/2, F_s/2)$. The sampling period is T and the time shift between the real and the imaginary data set is dT <0, T/2>. The resulting sets of samples are:

$$Rn = \{ A \cos(2\pi F_a n T + \Phi) \} \qquad (4)$$

$$In = \{ A \sin(2\pi F_a (n T + dT) + \Phi) \}$$

Using $F_a=F_s+ Fv$, to convert F_a in the base band, we receive:

$$Rn = \{ A \cos(2\pi F_v n T + \Phi) \} \qquad (5)$$

$$In = \{ A \sin(2\pi F_v (n T + dT) + \Phi + 2\pi F_s dT)\}$$

The term $2\pi F_s dT$ gives us the origin and phase of the aliased signals. Using $\beta = 2\pi F_s dT$ and making the set of samples of two harmonics signals with base band

frequencies F_v, $-F_v$, amplitudes A_1, A_2 and phases Φ_1, Φ_2, we receive (6):

$$Rn = \{ A_1 cos(2\pi F_v nT + \Phi_1) + A_2 cos(-2\pi F_v nT + \Phi_2) \} \quad (6)$$

$$In = \{ A_1 sin(2\pi F_v (nT + dT) + \Phi_1) + A_2 sin(-\pi F_v (nT + dT) + \Phi_2) \}$$

If we compare (5) and (6), we receive the resulting aliased signals:

$$A_1 = A\ cos(\beta/2) \quad (7)$$

$$A_2 = A\ sin(\beta/2)$$

$$\Phi_1 = \Phi + \beta/2$$

$$\Phi_2 = -\Phi - \beta/2 + \pi/2$$

So the signal with frequency F_a aliased in two positions, with frequencies F_v and $-F_v$ and amplitudes and phases given by (7). The special cases are the *pure-complex data* or *Redfield data*, when the aliased signal occurs at one frequency only.

Pure-complex data, dT=0: So $\beta = 0$ and from (7) $A_1=A$, $A_2=0$ and $\Phi_1=\Phi$. The aliased signal occurs at the frequency $F_v = F_a - F_s$ with the phase Φ.

Redfield data, dT=1/2F_s. So $\beta=\pi$ and $A_1=0$, $A_2=A$, $\Phi_2=-\Phi$. The aliased signal occurs at the frequency F_s-F_a with the phase $-\Phi$.

Complex-dT data, dT (0,1/2F_s). Aliased signals occur at two frequencies F_a-F_s, F_s-F_a with phases and amplitudes according to (7).

In Fig.3. the spectrum of the aliased signal with frequency 1.1 [F_s/2] is illustrated. The influence of the time shift on the aliased data explains all differences between the resulting data. In principle, it is possible to increase the sampling frequency to prevent the aliasing. However, this conflicts with the need to keep the data size and the load of computations off line at a minimum. So the effect of attenuated signals in the transient band of the filter should be taken into consideration, especially in the case of the high dynamic range. The conclusion of this analysis is that the *complex-dT* data should be avoided even though they may simplify the hardware design. The penalty that the aliased signals occur in two positions is very serious.

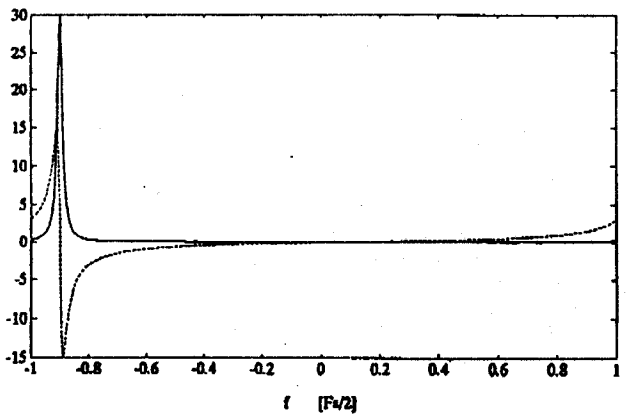

(3a)

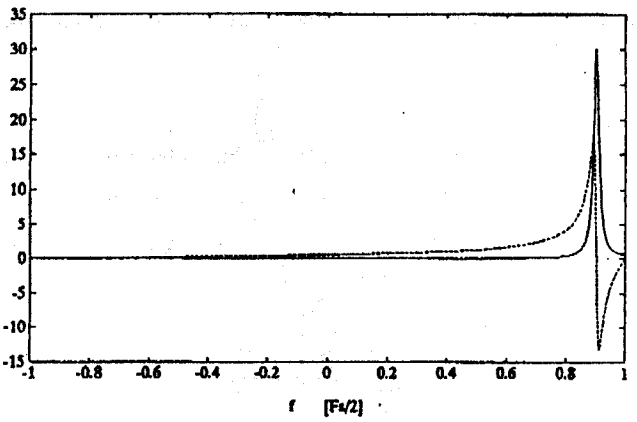

(3b)

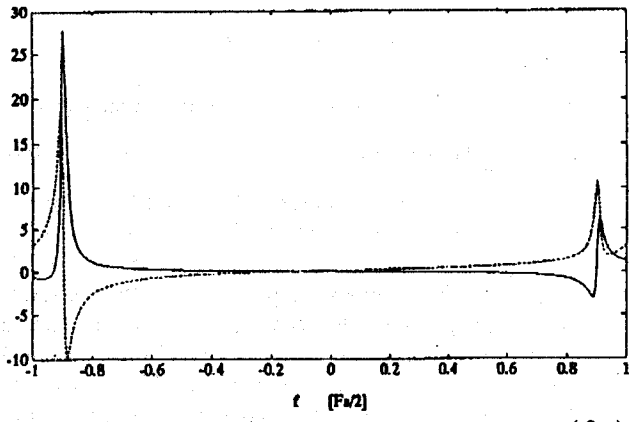

(3c)

Fig. 3. Influence of the time shift dT between real and imaginary samples on the resulting spectrum. Input harmonic signal with frequency 1.1 [F_s/2] and exponential envelope. Solid line - real part of output spectrum, dashed line - imaginary part.
a) Pure-complex data, dT=0.
b) Redfield data, dT=0.5T.
c) Complex-dT data, dT=0.1T

This analysis is also a simple explanation why the spectral distortion is different for *Redfield* and *pure-complex data*, and which data type is better according to the input signal and analyzed band. Generally, it can be said that the *pure-complex data* is mostly better. The aliasing can also explain why it is possible to do the data decimation without lowpass filtering in the case of *Redfield data*. What happens in case of sample decimation is illustrated in Fig.4.

5. Narrow lowpass filter

The used lowpass filter may be tunable within a broad band range (up to 10^5) together with the corresponding decimation of the samples. During the sample decimation, the aliasing of stop bands takes place and the steepness of the frequency response is taken according to the decimated samples and the resulting spectral width. This increases the demand on the frequency response and the lowpass filter must be nearly

ideal. The narrower the pass band, the greater the difficulty in

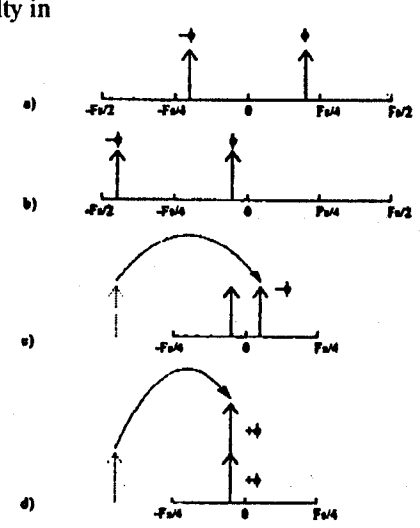

Fig.4 Spectral representation of sample decimation to receive Redfield data. a) Spectrum of the input signal b) After DQD with $F_s = 4F_c$ c) Simple sample decimation, result pure-complex data d) Sample decimation to receive Redfield data.

obtaining a good frequency response with the classical filter design [13]. One filter can not satisfy the need, a cascade of filters must be used. The HP3582 spectral analyzer shows the first solution to the problem. It is the cascade of IIR filters. Each filter narrows the pass band twice and decimates the sample twice. One VLSI was used and the computing was made in the time-sharing. The IC counts two responses during one sample period and the sampling frequency may be up to 40 kHz.

Finally, a better algorithm has been found which is based on the cascade of two different filters. This solution is used, for example, in HARRIS IC. The first filter in the cascade is called the *High Order Decimation Filter* (**HDF**) and is used for fundamental narrowing the translated band. It is responsible for the tuning and its influence on the steepness of the resulting frequency response is mostly not remarkable. The second filter is the FIR filter. Its narrowing of the translated band is small, mostly fixed, and its frequency response determines the shape of the resulting frequency response.

The HDF filter is a cascade of some (one to five) **COMB** filters. The COMB filter is a simpler digital filter, with only one parameter k, which is described as follows:

$$y(n) = SUM\,[x(n-i)] \qquad i \langle 0,k-1 \rangle \qquad (8)$$

$$H(z) = (1-z^{-k})/(1-z^{-1})$$

$$|H(\Omega)| = \sin(k\,\Omega/2) / \sin(\Omega/2) \qquad \Omega \langle 0,2\pi \rangle$$

Its frequency response for $k = 10$ is shown in Fig 5a. The solid line is one COMB filter, the dashed line is a cascade of two COMB filters. If the sample decimation by k is made at the output, the output band corresponds to the input range $\langle 0,\ 2\pi/k \rangle$ and the frequency response is:

$$|H(\Omega_d)| = \sin(\Omega_d/2) / \sin(\Omega_d / 2k) \qquad \Omega_d \langle 0,2\pi \rangle \qquad (9)$$

For a large k, where $\Omega_d/2k \Rightarrow 0$ and $\sin(\Omega_d/2k) \Rightarrow \Omega_d/2k$, the relation becomes simpler:

$$|H(\Omega_d)| = 2k\ \sin(\Omega_d/2)\ /\Omega_d \qquad (10)$$

On this assumption, the frequency response of the COMB filter is always the same with regard to the decimated samples. The coefficient k determines the fundamental narrowing of the frequency band. However, the output frequency response does by no means come up to the expectations regarding the characteristic of an ideal lowpass filter - Fig.5b. The solid line is one COMB filter, the dashed line is a cascade of five COMB filters. The lines marked A give the attenuation of aliased signals. Thus, we have to consider another narrowing of the translated band by the FIR filter.

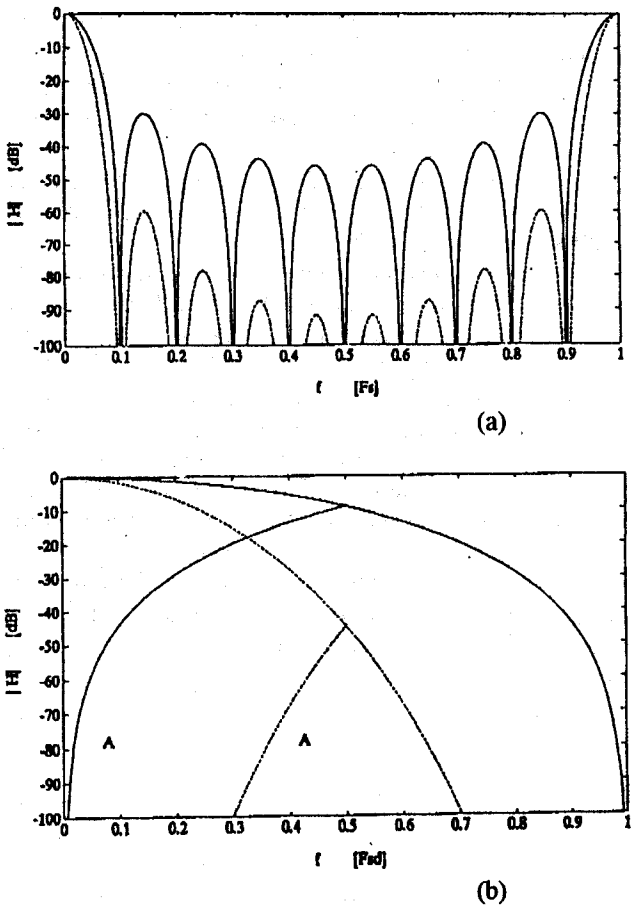

Fig.5. Frequency response of COMB filter, k=10.
a) According to the input samples. Solid line - one COMB, dashed line - two COMB.
b) According to the decimated samples. Solid line - one COMB, dashed line - five COMB. Lines denoted by A - the aliased band ($F_{sd}/2$, F_{sd}).

The frequency response of the FIR filter determines the resulting frequency response. From this point of view, the narrowing of the frequency band by the FIR filter may be small, to achieve a good steepness

between the pass band and the stop band. On the other hand, the frequency response of the HDF filter is bad, there are attenuations in the resulting passband and aliasing. The distortion is the biggest at the border of the resulting spectral width. The attenuation due to the COMB filter in the passband is given by:

$$-20\ N\ \log_{10}(\sin(\alpha)/\alpha) \quad [\text{dB}] \qquad (11)$$

where $\alpha=\pi/(2K_{FIR})$, K_{FIR} is the translated band narrowing in FIR and also the sample decimation at the output of FIR, and N is the number of stages of the COMB filter. This attenuation can be overcompensated by the FIR response. More serious is the aliasing. The aliased signals at the border are attenuated:

$$-20\ N \log_{10}(\sin(\pi-\alpha)/(\pi-\alpha)) \ [\text{dB}] \qquad (12)$$

From this point of view, the optimum narrowing of the passband in the FIR filter ranges from 4 to 6.

6. Special HARRIS DSP for digital receiver design

Some years ago, the design of the digital receiver was limited by the capabilities of the hardware. Either the hardware had to be very much complicated, or the sampling frequency had to be low, or both. Mostly, the analog quadrature detection was used and also the digital filtering in real time was a problem. All changed by using HARRIS DSP:

HSP43220 - *Decimating Digital Filter*
. Single chip narrow band filter: HDF + FIR
. Input: 16 bit 2's complement, F_s up to 33 MHz
. HDF: 5 COMB filters, decimation <16 ,1024>
. FIR: 20 bit coefficients, to 512 taps, programmable
. Output: 24 bit
. Control: parallel port
. 84 pin PGA and PLCC

HSP45116 - *Numerically Controlled Oscillator/Modulator*
. Input: 2* 16 bit (real + imag), F_s up to 33 MHz
. Output: 2* 16 bit
. 32 bit frequency control (0.008 Hz resolution at 33 MHz)
. 16 bit phase modulation
. Spurious frequency components < -90dB
. 145 pin PGA

HSP50016 - *Digital Down Converter*
. Single chip synthesizer, quadrature detector and lowpass filter
. Input: 16 bit, F_s up to 70 MHz
. 32 bit frequency control
. Spurious free dynamic range through modulator > 102dB
. chirp frequency mode
. filter HDF + FIR, FIR fix frequency response, decimation four times
. HDF: decimation <64 ,128000>
. Identical lowpass filters for real and imag part
. Passband ripple < 0.04dB
. Stopband Attenuation > 106dB
. Filter -3dB to -102dB shape factor < 1.5
. Output: serial, 16 to 38 bit
. Control: serial, 40 bit words
. 44 lead PLCC

HSP43220 is an ideal solution to the narrowband lowpass filter. The input and output data are parallel, IC is full programable - number of COMB filters, coefficients of FIR filter, whether both HDF and FIR filter or only one will be used, type of output data and magnification. Two of these IC and DQD (HSP45116 or simple solution based on XILINX for frequency conversion $F_s/4$) form the digital receiver.

HSP50016 is a perfect solution to the digital receiver in one IC that can be applied in many areas. Using this IC, limitation of ADC take place at present. It is not possible to take advantage of the high F_s and of the high input dynamic range of HSP50016 at the same time. For this we will need at least a 12 bit ADC with F_s of up to 70 MHz. Some limitation of this IC is the maximal translated band, that is $F_s/100$. To overcome this limitation, if F_s is limited by ADC, it is possible to use the interpolation of zeroes. The maximal translated band can also be limited by the speed of the serial communication of the output data.

7. Measurement

The next measurement are done with our home made digital receiver designed as acquisition unit for nuclear magnetic resonance spectroscopy and tomography. The digital receiver is based on HSP50016. The hardware is very simple - exchangeable ADC, HSP50016 and ADSP2101 with external RAM. The carrier frequency can be arbitrary and the limitation of this receiver is given by ADC (Analog Devices AD827 12 bit, 10 MS/s). In Fig.6 to 8. the application of this acquisition unit is illustrated. The dynamic range of receiver is limited by ADC, so the amplitude unit is taken relative to the full scale signal of ADC.

The measurement of the weak signal in the presence of strong one is in Fig.6 a,b. The strong signal is output from frequency synthesizer PTS500, amplitude is 6 dB below the full scale of ADC, and frequency is 2.5 MHz. The weak signal is attenuated output from Tesla generator BM546, frequency 2.50052 MHz. The sampling frequency was 10 MHz, the mixing frequency was 2.5 MHz and the data size was 8 K complex word. Fig. 6 b uses the linear scale along the y axis. This is useful when we analyze weak signals in the presence of a strong, disturbing one. The separate measurement of the strong and weak signal is in Fig.6 a,b. We can see, that no one of the applied synthesizers is the source of clean harmonic signal.

The both synthesizers are measured in Fig. 7. Carrier frequency is 2.5 MHz and sampling frequency is 10 MHz. Amplitude is 6 dB below the full scale level. The synthesizer PTS500 is in Fig. 7 a,c and the Tesla generator BM546 is in Fig. 7 b,d. On Fig. 7 c,d we can see the phase noise, the rest after substraction the signal on the carrier frequency.

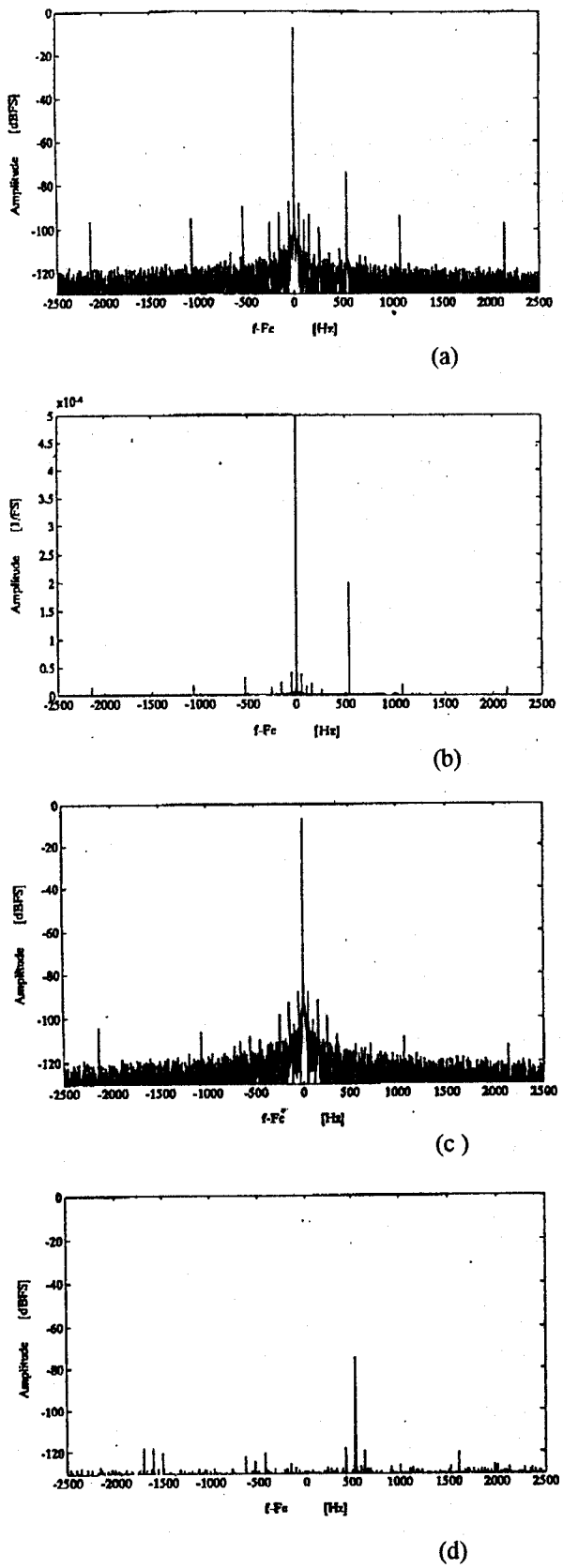

Fig.6. Measurement of weak signal (Tesla generator BM546, frequency 2.50052 MHz) in the presence of strong one (synthesizer PTS500, frequency 2.5 MHz)
a, b) Both signals
c) Only strong signal
d) Only weak signal

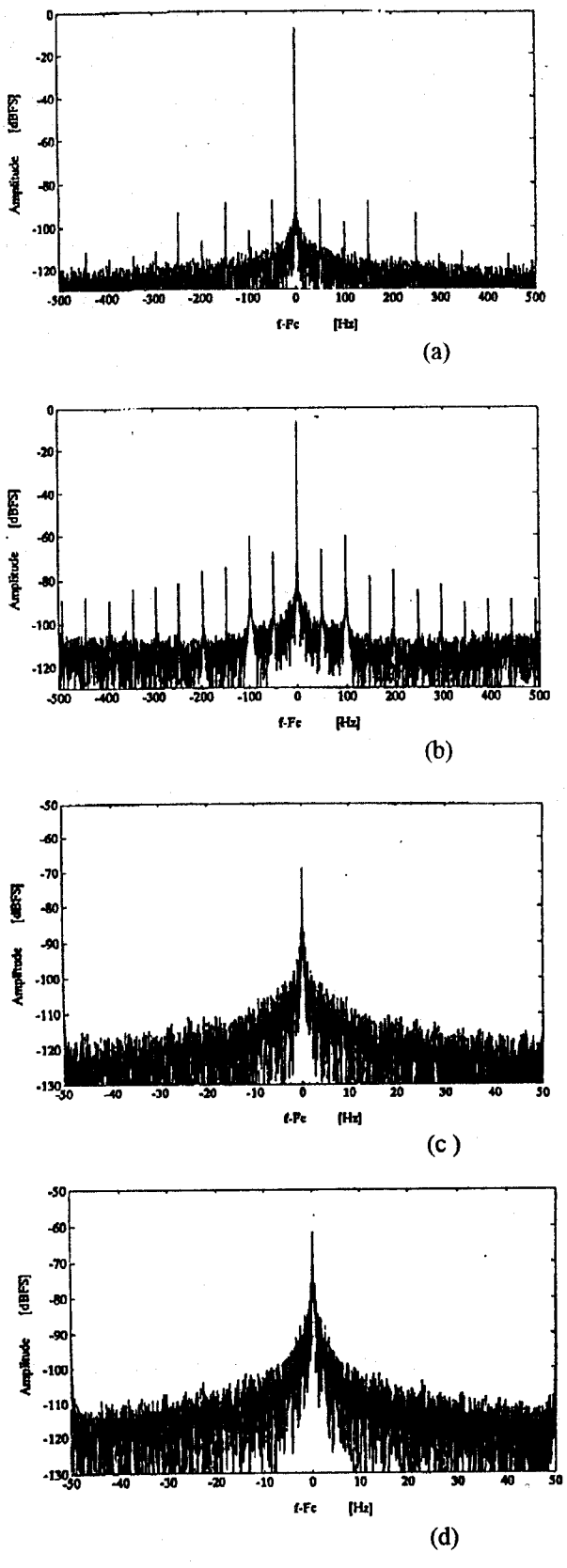

Fig.7. Purity of output signals from PTS500 synthesizer (a, c) and Tesla generator BM546 (b,d). Output frequency is 2.5 MHz.
c, d) The rest after subtracting the carrier frequency

The receiver ghost signals are measured in Fig. 8. Carrier frequency is 2.750 MHz, mixing frequency is 2.750320 MHz, sampling frequency is 10 MHz, and the Kaiser-Bessel window vas applied. From result we can see, that the digital receiver has neither the dc error signal nor signals aliased round the zero frequency.

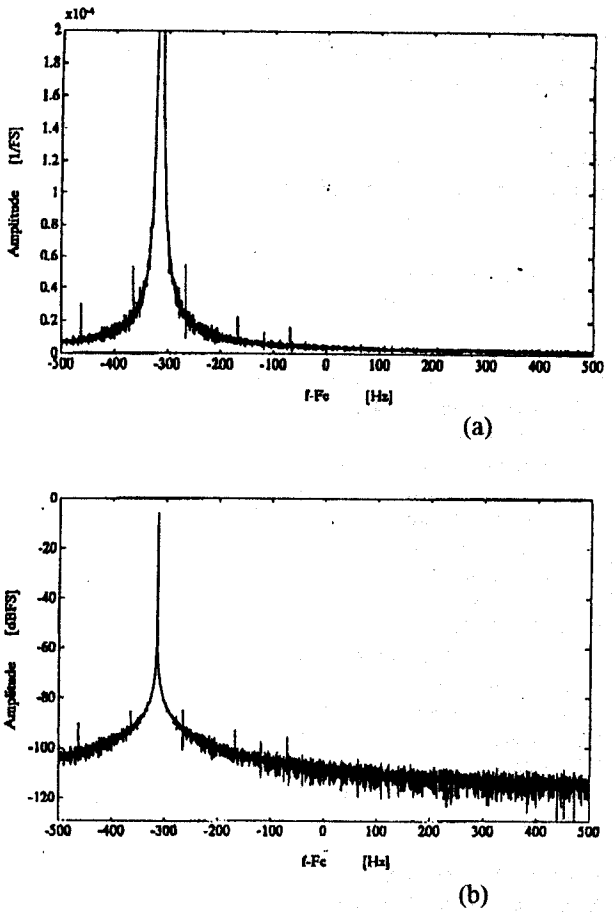

Fig.8. Measurement the dc error signal and aliasing round the zero frequency.

8. Conclusion

The bandpass signal analysis has to be based on digital receiver. The digital receiver enables us to achieve the high dynamic range, nearly ideal SNR, narrow band filtering, simple tuning, phase linearity, and to eliminate distortion and ghost signals. The application of Harris DSP simplifies the hardware design and nearly all problems of digital signal processing are eliminated. But the top parameters depend also on ADC design and proper application. The limitation of the dynamic range in the case of the digital receiver is mostly no longer the noise, but the mixing products and spurious signals. Unfortunately, the source of this signals may be also the ADC. So the design of ADC unit is the other key to the receivers performance.

9. Acknowledgements

This work was supported by the Grant Agency of the Czech Republic (102/96/1509 and 102/94/1270).

Appendix

An example of FFT for a complex signal with the time shift between real and imaginary samples, MATLAB.

```
tau=0.1;          % time shift, <0,0.5> relative to sampling
                    period
fx=1.1;           % frequency of input signal, relative to Fs/2
fi=0;             % phase of input signal
ta=30;            % time constant of exponential envelope
NN=1024;          % number of samples
t=0:1:NN-1;       % time
% input signal
Rn = exp(-t/ta).*cos(pi*fx*t + fi);
In = exp(-(t+tau)/ta).*sin(pi*fx*(t+tau) + fi);
Rn(1) = 0.5*Rn(1);
if(tau==0)
    In(1) = 0.5 * In(1);
end
% FFT of two real functions Rn, In
y=Rn + j*In;
y=fft(y);
yr=(real(y(2:NN))+real(y(NN:-1:2)) + ....
    j*(imag(y(2:NN))-imag(y(NN:-1:2))))/2;
yi=(imag(y(2:NN))+imag(y(NN:-1:2)) + ....
    j*(real(y(2:NN))-real(y(NN:-1:2))))/2;
yr = [real(y(1)) yr];
yi = [imag(y(1)) yi];
% spectrum of the input signal
f = [ [0:2/NN:1] [(-1+2/NN):2/NN:-2/NN] ];
y= yr + j*exp(-j*pi*f*tau) .*yi;
% zero frequency to centre
y=fftshift(y);
%result
x=-1:2/NN:(1-2/NN);
plot(x,real(y),x,imag(y))
```

References:

[1] N.A.PENDERGRASS, J.S.FRANBACH: A High-Resolution, Low-Frequency Spectrum Analyzer. HP Journal September 1978, p. 2-14, (1978)

[2] G.C.NASCIMENTO,M.ENGELSBERG,R.E.SOUZA: Digital NMR imaging Systems for Ultralow Magnetic Fields. Meas. Sci. Technol. 3, p.370-375, (1992)

[3] C.OLMSTEAD AND M. PETROWSKI: Single Chip Digital Down Converter in Communications Applications. Proc. of ICSPAT'93, p.636-640, (Santa Clara 1993)

[4] M.PETROWSKI: Single Chip Digital Down Converter Architecture. Proc. of ICASSP'93, p.349-355, (Minneapolis 1993)

[5] MEHLKOPF AND J.H.DEN BOEF, Abstract VII SMRM Meeting, p.857, (San Francisco, 1988)

[6] R.S.STORMONT et. al., Abstract VIII SMRN Meeting, p. 982, (Amsterdam, 1989)

[7] M.KASAL, J.HALÁMEK, V. HÚSEK, M.VILLA, U.RUFFINA AND P.COFRANCESCO: Signal processing in transceivers for NMR/MRI. Rev. Sci. Instr. 65, p.1897-1902, (1994)

[8] J. HALÁMEK, V. VONDRA AND M. KASAL: The elimination of baseline distortions induced by audio filters. J.Magn.Res. A110, p.194-197, (1994)

[9] J. HALÁMEK, M.KASAL, I.KREJČÍ, P.COFRANCESCO, M. VILLA: Requirements and implementation of a high dynamic range ZOOM FFT: system response analysis. Proc. of ICSPAT'93, p.349-352, (Santa Clara, 1993)

[10] M. VILLA, F. TIAN, P. COFRANCESCO, J. HALÁMEK, M.KASAL: High-resolution digital quadrature detection. Rev. Sci. Instr. 67, p.2123-2129, (1996)

[11] KELLER AND U. HAEBERLEN: Generalization of the Redfield-Kunz Treatment of Quadrature Phase Time Data. HP Journal December 1988, p. 74-75, (1988)

[12] REDFIELD AND S.D.KUNZ, J.MAGN.RES. 19, p.250, (1975)

[13] R. MAJIDI-AHY, H. HILL, G. ZDASIUK: Implementation, limitation and application of real-time decimating FIR digital filters. ICSPAT'92, p.133-136, (Boston, 1992)